

PAPER

Calculation magnetic dipole moments, electric quadrupole moments and form factors for some Ti isotopes

To cite this article: Ahmed H Ali and Ali A Alzubadi 2020 *Phys. Scr.* **95** 105306

View the [article online](#) for updates and enhancements.

Calculation magnetic dipole moments, electric quadrupole moments and form factors for some Ti isotopes

Ahmed H Ali^{1,3}  and Ali A Alzubadi²

¹Department of Medical Physics, College of Applied Science, University of Fallujah, Iraq

²Department of Physics, College of Science, University of Baghdad, Baghdad, Iraq

³Biotechnology and Environmental Center/University of Fallujah, Iraq

E-mail: dr.ahmedphysics@uofallujah.edu.iq

Received 14 June 2020, revised 17 September 2020

Accepted for publication 23 September 2020

Published 30 September 2020



Abstract

This paper presents calculations of the magnetic moments, the quadrupole moments, and the form factors of a number of titanium isotopes as determined using the shell model space. The calculations of the shell model have adopted the model space (MS) with core-polarization effects, which were included for two types of effective g factors and different effective charges. The wave functions are generated using the harmonic oscillator potential (HO) with size parameters b , which for these isotopes are calculated. The one body density matrices (OBDM) for these isotopes were obtained using the NuShellX@MSU code, which used an adopted *fpd6* interaction and *fp* model space. Reasonable results are obtained that show the collapse of the magicity property at neutron number $N = 28$.

Keywords: electric quadrupole, magnetic moment, form factor, interaction, effective charges, shell model

(Some figures may appear in colour only in the online journal)

1. Introduction

Calculations to determine the magnetic dipole moments, electric quadrupole moments, and form factors, give extensive information about the structure of nuclear states, nuclear moments, nuclear deformation, and the way charge is distributed around the atom. Electromagnetic moments are considered to be amongst the most basic probes one can use to obtain information about the nuclear structure throughout the entire nuclear chart. The magnetic moments of nuclei are highly sensitive to the orbits occupied by the valence nucleons, where magnetic moments offer a perfect test of the purity of a specific configuration mixing shell model [1]. The static electric quadrupole moments ($Q.M$) of nuclei can provide a measure of their nuclear deformation. The differences in their magnitudes and signs vary as a function of the charge number, A , and mass and atomic number, Z , are sensitive measures of the many-particle structures of the nuclear wave functions [2]. Microscopic theory can be used to calculate the

quadrupole moment of a nucleus [3]. The types of the quadrupole moments, which is a measure of the deformation of the nucleus, can be categorised as oblate ($Q.M < 0$) or prolate ($Q.M > 0$). In the nuclear state, the magnetic moment of a nucleus with spin I and with a nuclear gyromagnetic ratio (g) is given by $\mu = gI\mu_N$. The nuclear magneton μ_N is a unit of experimental magnetic moments but experimental methods tend to act as measures of the nuclear g factor. In both cases, however, this represents a way to calculate the unknown spin of an exotic nuclear state. This can be achieved by comparing the experimental magnetic moment to model calculations or by comparing the values of a similar state to the measured values. The *fpd6* interaction for two-body was derived for nuclei in the lower part of the *0f1p* shell using two-body matrix elements to 61 binding and fitting semi-empirical potential forms and excitation energy data in the mass range $A = 41$ to 49. Excellent reproduction of ground state magnetic moments and quadrupole moments is gained with *fpd6* interactions [4]. Elastic electron-nucleus scattering can be

used as a handy tool to investigate the shape and size of stable nuclei [5]. Electron scattering calculations for the nucleus employ the exact phase-shift analysis of the Dirac equation. This method agrees with the so-called distorted wave Born approximation (DWBA) [6].

In the present work, the magnetic dipole moments, the electric quadrupole moments, and elastic longitudinal electron scattering form factors are calculated for selected Ti isotopes using the *fp* shell model space with a *fpd6* two-body effective interaction [4]. The Ti isotopes investigated in the present work are from the very interesting region near $Z = 20$ and between the neutron shell closures at $N = 20$ and 28. The ^{44}Ti isotope is of particular interest since, in contrast to other Ti isotopes, it is predicted to have a dominant $^{40}\text{Ca} + \alpha$ cluster structure in its ground state. The calculated results were compared to available experimental data. These Ti isotopes are composed of a ^{40}Ca core and active valence nucleons distributed in the *fp*-shell. The core-polarization (CP) effects are included through effective g factors and effective charge.

2. Theory

For electric 2^L pole transitions, the operator is defined [7] as:

$$O(ELM) = \int \rho^{op}(r) r^L Y_{LM}(\hat{r}) dr, \quad (1)$$

$\rho^{op}(r)$ denotes the charge densities that are considered to be operators.

The nucleons are considered to be nonrelativistic point particles with a charge and/or magnetic moment. Therefore, one may write the charge density operator as

$$\rho^{op}(r) = \sum_{k=1}^A e(k) \delta(r - r(k)), \quad (2)$$

or the charge density as

$$\begin{aligned} \rho(r) &= \langle \psi | \rho^{op}(r) | \psi \rangle \\ &= \sum_{k=1}^A e(k) \delta(r - r(k)) \psi^*(r(1), \dots, r(A)) \\ &\quad \times \psi(r(1), \dots, r(A)) dr(1) \dots dr(A), \end{aligned} \quad (3)$$

where $e(k)$ denotes the charge of nucleon k , i.e., $e(k) = 0$ for a neutron and $e(k) = e$ for a proton. Substituting equation (2) in to equation (1) gives the operator for an electric transition [7]

$$\hat{O}(ELM) = \sum_{k=1}^A e(k) r^L(k) Y_{LM}(\hat{r}(k)). \quad (4)$$

The operator for a magnetic transition is

$$\begin{aligned} \hat{O}(MLM) &= \sum_{k=1}^A \mu_N \left[g^s(k) s(k) + \frac{2g^l(k)}{L+1} l(k) \right] \\ &\quad \nabla(k) r^L(k) Y_{LM}(\hat{r}(k)), \end{aligned} \quad (5)$$

where the orbital g -factor is introduced as $g^l = 1$ for a proton, and $g^l = 0$ for a neutron.

The second term in equation (5), resulting from the convection current, contains the operator $l(k) = r(k) \times p(k)/\hbar$, which does not act on $\nabla(k) r^L(k) Y_{LM}(\hat{r}(k))$, but only on the

nuclear wave functions when the matrix element is taken [7] and the μ_N denotes, to the unit of the nuclear magnetic moment, i.e., the nuclear magneton, while M_p denotes the proton mass.

$$\mu_N = \frac{e\hbar}{2M_p c} = 1n.m = 0.15 e.f.m, \quad (6)$$

The final expression for magnetic 2^L pole moment is:

$$\begin{aligned} \mu^L &= \langle JJ | \sum_{k=1}^A \mu_N \{ \nabla(k) r^L(k) Y_{L0}(\hat{r}(k)) \} \\ &\quad \left\{ g^s(k) s(k) + \frac{2g^l(k)}{L+1} l(k) \right\} | JJ \rangle, \end{aligned} \quad (7)$$

For the case of $L = 1$ equation (7) assumes a particularly simple form after substitution of $\nabla r^1 Y_{10} g^l = \sqrt{3/4\pi} l_z$. The magnetic dipole moment μ of a state of total angular momentum J from [7].

$$\mu = \sqrt{\frac{4\pi}{3}} \sqrt{\frac{J}{(J+1)(2J+1)}} \langle J || \hat{O}(m1) || J \rangle \mu_N, \quad (8)$$

For $J = 1$, the μ is defined by the $m1$ operator as [8]

$$\mu = \sqrt{\frac{4\pi}{3}} \begin{pmatrix} J_i & 1 & J_i \\ -J_i & 0 & J_i \end{pmatrix} \langle J || \hat{O}(m1) || J \rangle \mu_N, \quad (9)$$

where $\langle J || \hat{O}(m1) || J \rangle$, the operator of the magnetic transition, μ_N is taken from equation (6).

The orbital and spin free nucleon g factors for a proton are $g^l(p) = 1$ and, $g^s(p) = 5.585$, and for neutron, they are $g^l(n) = 0$, and $g^s(n) = -3.826$ [7].

In nuclear physics, the quadrupole moment (in the state $M = J$) is referred to the spectroscopic or static quadrupole moments [8]:

$$Q(J, M = J) = \sqrt{\frac{16\pi}{5}} \sqrt{\frac{J(2J-1)}{(J+1)(2J+1)(2J+3)}} \langle J || \hat{O}(E2) || J \rangle, \quad (10)$$

where the electric transition operator $\hat{O}(E2)$ is defined from equation (4) [9].

The nuclear matrix element is $\langle J || \hat{O}(E2) || J \rangle$ where J_i is represents the initial nuclear states and J_f represents the final nuclear states for multipolarity (λ) is equal to the products of the single-particle matrix elements and the one-body density matrix (OBDM) [9]

$$\langle J_f || \hat{O}(\lambda) || J_i \rangle = \sum_{jj'} OBDM(J_i, J_f, j, j', \lambda) \langle j' || \hat{O}_j(\lambda) || j \rangle, \quad (11)$$

The single-particle states are represented by the difference between j' and j for the states of the shell model. The effective charges ($e^{eff}(t_z)$) only includes the model space (MS) of the electric matrix element $M(EJ)$

$$M(EJ) = \sum_{t_z} e^{eff}(t_z) \langle J_f || \hat{O}_2(\vec{r}, t_z) || J_{iMS} \rangle \quad (12)$$

Table 1. The calculated the magnetic dipole moments (μ) in units μ_N using (a) free g factors [7] and (b) effective g factors [9] for the $^{43,44,45,46,47,48,49,50,52}\text{Ti}$ isotopes. The results were compared with experimental data (μ_{exp}) taken from [13].

^{22}Ti N, A	J^π	$b(\text{fm})$	$\mu(\mu_N)_{\text{theo}}$ <i>free (a)</i>	$\mu(\mu_N)_{\text{theo}}$ <i>eff. (b)</i>	$\mu(\mu_N)_{\text{exp}}$
21, 43	$19/2^-$	1.960	7.378	7.6317	+7.22 (1)
22, 44	2^+	1.966	1.02	1.0905	+1.0 (3)
23, 45	$7/2^-$	1.972	-0.35	-0.1181	0.095 (2)
24, 46	2^+	1.978	0.66	0.7386	+0.99 (5)
25, 47	$5/2^-$ stable	1.983	-0.93	-0.7323	-0.78848 (1)
26, 48	2^+	1.989	0.63	0.6973	+0.78 (4)
27, 49	$7/2^-$ stable	1.995	-1.25	-1.0060	-1.1041 (1)
28, 50	2^+	2.00	2.27	2.2722	+2.89 (15)
30, 52	2^+	2.01	0.75	0.8242	+1.7 (4)

⁴ Free g factors. ($g_s^p = 5.586$, $g_s^n = -3.826$, $g_l^p = 1.000$, $g_l^n = 0.0$) [7].

⁵ Effective g factors. ($g_s^p = 5.055$, $g_s^n = -3.19$, $g_l^p = 1.06$, $g_l^n = 0.0$) [9].

The effective charges was calculated via [8]:

$$e^{\text{eff}(t_z)} = Z/A - 0.32(N - Z)/A - 2t_z \times [0.32 - 0.3(N - Z)/A], \quad (13)$$

The quadrupole moment (Q, M) for $J_f = J_i$ is [9]:

$$\begin{aligned} Q(J=2) &= \sqrt{\frac{16\pi}{5}} \begin{pmatrix} J_i & J & J_i \\ -J_i & 0 & J_i \end{pmatrix} \langle J || \hat{O}(E2) || J \rangle \\ &= \sqrt{\frac{16\pi}{5}} \begin{pmatrix} J_i & 2 & J_i \\ -J_i & 0 & J_i \end{pmatrix} M(EJ) \end{aligned} \quad (14)$$

Longitudinal electron scattering operator is defined as [10]

$$\hat{L}_{JM}(q) = \int j_J(qr) Y_{JM}(\Omega_r) \hat{\rho}(\vec{r}) d^3r$$

The longitudinal electron scattering form factor of the nucleus is defined as [10]:

$$|F(q)|^2 = \frac{4\pi}{z^2(2J_i + 1)} \sum_J \langle J_f || \hat{L}_J(q) || J_i \rangle^2, \quad (15)$$

From the shell model, the correction of the form factor by finite-size for the nucleon ($f.s.$) is $F_{f.s.} = \left[1 + \left(\frac{q}{4.33} \right)^2 \right]^{-2}$, the correction for the form factor of the center of mass of the nucleon (the lack of translational invariance) is calculated via $F_{c.m.} = e^{q^2 b^2 / 4A}$, where the b size parameter is the length parameter of the harmonic oscillator (HO), and A is the mass number [8].

3. Results and discussion

In the present work, the magnetic dipole moments ' μ ', the electric quadrupole moments ' Q, M ' and form factor ' F, F ' have been calculated for various Ti isotopes with different effective charges. In particular, ^{43}Ti ($N = 21; 19/2^-$), ^{44}Ti ($N = 22; 2^+$), ^{45}Ti ($N = 23; 7/2^-$, stable), ^{46}Ti ($N = 24; 2^+$), ^{47}Ti ($N = 25; 5/2^-$), ^{48}Ti ($N = 26; 2^+$), ^{49}Ti ($N = 27; 7/2^-$, stable), ^{50}Ti ($N = 28; 2^+$), and ^{52}Ti ($N = 30; 2^+$). The calculations were performed with a restricted fp shell model space which consisted of $1f_{7/2}$, $2p_{3/2}$, $1f_{5/2}$, $2p_{1/2}$ orbitals and ^{40}Ca as an inert core.

The one-body density matrix (OBDM) element was calculated via the NuShellX@MSU code [11], were performed using the $fpd6$ interaction [4] and with valence (frozen) protons are restricted to the $1f_{7/2}$ orbit and neutrons $N \geq 20$, which covered the $1f_{7/2}$, $2p_{3/2}$, $1f_{5/2}$, and $2p_{1/2}$ orbits. The CP effects were included through the effective g factors and the effective charge for fp model space. The size parameters b and the harmonic oscillator (HO) potential are adopted to calculate the radial wave functions of the single-particle matrix elements. The size parameters b of a number of the Ti isotopes were calculated via their mass number (A):

$b = \sqrt{\frac{\hbar}{M_p \omega}}$, where $\hbar \omega = 45A^{-1/3} - 25A^{-2/3}$ (M_p = mass of proton) [12].

3.1. Nuclear magnetic dipole moments

Magnetic dipole moments were calculated using both types of g -factor and the results compared with experimental data

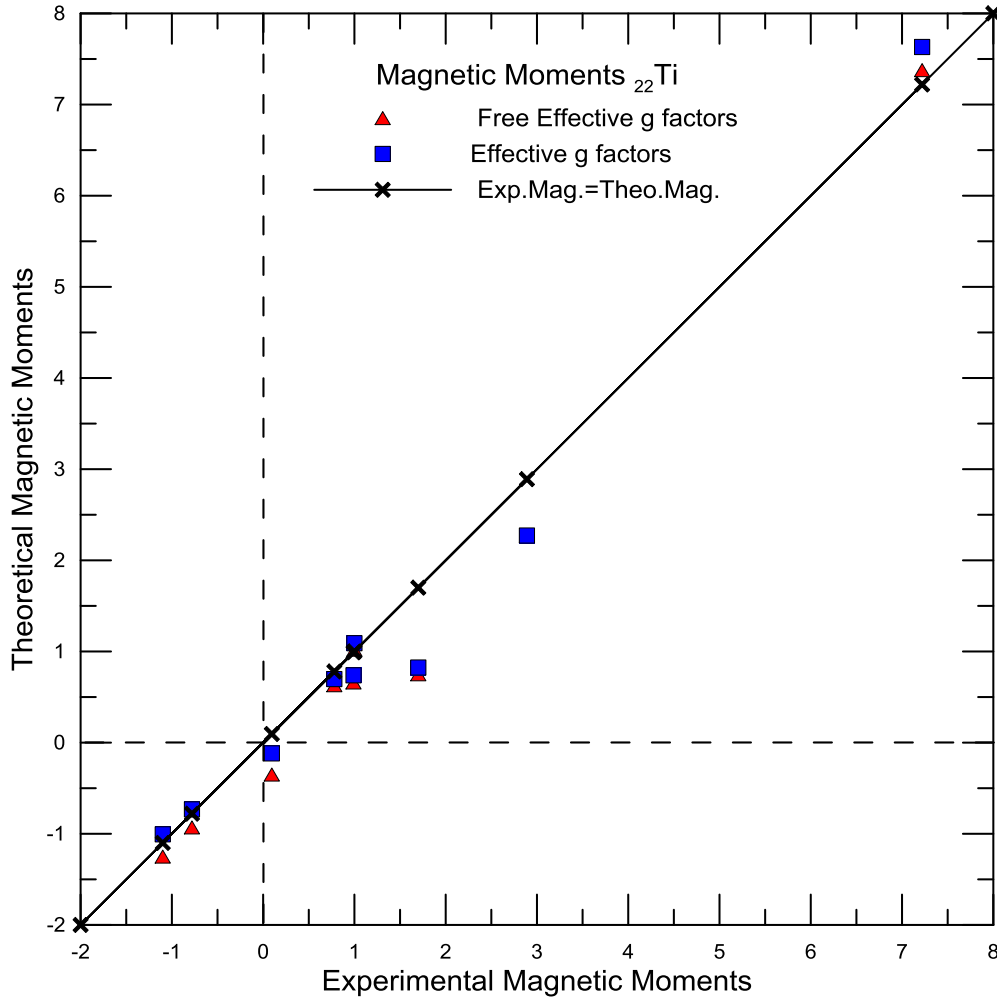


Figure 1. Comparison between theoretically calculated data and the experimental data taken from [13] for the $^{43,44,45,46,47,48,49,50,52}\text{Ti}$ isotopes. Scattering around $\mu_{\text{exp}} = \mu_{\text{theo}}$ is studied.

taken from [13]. The theoretical values of the magnetic dipole moment, μ_{theo} , for the ^{43}Ti ($J^\pi = 19/2^-$) isotope were calculated using free nucleon g factors ($g_s^p = 5.586$, $g_s^n = -3.826$, $g_l^p = 1.0$, $g_l^n = 0.0$) [7] and effective nucleon g factors ($g_s^p = 5.055$, $g_s^n = -3.19$, $g_l^p = 1.06$, $g_l^n = 0.0$) [9] which give $\mu = 7.378$, and $7.6317\mu_N$, respectively. These results are close to the experimental data $\mu_{\text{exp}} = 7.22 \pm 1 \mu_N$ [13]. The μ_{theo} calculated for the ^{44}Ti ($J^\pi = 2^+$) isotope using free g factors and effective g factors [9] give $\mu_{\text{theo}} = 1.02$ and $1.0905 \mu_N$, respectively. These results agreed with the reported experimental μ_{exp} [13]. The μ_{theo} determined for the ^{45}Ti ($J^\pi = 7/2^-$) isotope using the free g factor and effective g factors gave $\mu_{\text{theo}} = -0.35$ and $-0.1181 \mu_N$ which underestimated the experimental data [13]. The theoretically determined μ_{theo} for the ^{46}Ti ($J^\pi = 2^+$) isotope using free g factors and effective g factors gave $\mu_{\text{theo}} = 0.66$ and $0.7386 \mu_N$, predictions which are still reasonably close to the experimental data [13]. The theoretically determined μ_{theo} for the ^{47}Ti ($J^\pi = 5/2^-$, stable) isotope using free g factors was $\mu_{\text{theo}} = -0.93 \mu_N$, which underestimated μ_{exp} [13], while using effective g factors [9] is in

good agreement with the experimental data [13]. The theoretically determined value of μ_{theo} for the ^{48}Ti ($J^\pi = 2^+$) isotope using free g factors, was close to μ_{exp} [13], while the result using effective g factors was in good agreement with the experimental data [13]. The μ_{theo} calculate for the ^{49}Ti ($J^\pi = 7/2^-$, stable) isotope using the free g factors was close to the experimental data [13], and in good agreement with experimentally determined magnetic moments [13] when the effective g factors were used. The μ_{theo} for the ^{50}Ti ($J^\pi = 2^+$) isotope with the free g factors and the effective g factors both underestimated the experimental data [13]. The μ_{theo} for the ^{52}Ti ($J^\pi = 2^+$) isotope using the free g factors and the effective g factors underestimated the experimental data [13]. To illustrate the above in a more straightforward manner, the calculated results are tabulated in table 1 and illustrated in figure 1 in comparison with the appropriate experimental data. It may be noted that the deviation between the calculated and the experimental data is greatest when using the free nucleon g factors, whereas the effective nucleons g factors were in agreement with experimental for most isotopes.

Table 2. The theoretical calculated values of the quadrupole moments $Q.M_{th}$ (units of efm^2) for the $^{43,44,45,46,47,48,49,50,52}\text{Ti}$ ($Z = 22$) isotopes. The experimental electric quadrupole moments (measured) $Q.M_{exp}$ are taken from [13]. Calculations used the *fpd6* interaction [4], B-M effective charges [14], conventional effective charges Con ($e_p = 1.3 e$, $e_n = 0.5 e$) [15], and standard effective charges ST ($e_p = 1.36 e$, $e_n = 0.45 e$) [16], from the NushellX program Nu ($e_p = 1.5 e$, $e_n = 0.5 e$) [17], Emp.1 ($e_p = 1.23 e$, $e_n = 0.54 e$) and Emp.2 effective charges ($e_p = 1.01 e$, $e_n = 0.1 e$).

^{22}Ti N, A	state J^π	Eff. charge e_p, e_n	$Q.M_{th}$ (efm^2)	$Q.M_{th}$ (efm^2) CON	$Q.M_{th}$ (efm^2) ST	$Q.M_{th}$ (efm^2) Nu	$Q.M_{exp}$ (efm^2)
21, 43	$19/2^-$	B-M 1.19, 0.85	-27.35	-25.00	-25.27	-27.91	33±8
		Empe.1	-24.39				
		Empe.2	-16.07				
22, 44	2^+	B-M 1.18, 0.82	-21.62	-19.46	-21.62	-21.62	
		Empe.1	-19.13				
		Empe.2	-12.00				
23, 45	$7/2^-$	B-M 1.17, 0.80	-12.30	-10.01	-9.77	-10.82	1.5±15
		Empe.1	-10.11				
		Empe.2	-5.02				
24, 46	2^+	B-M 1.16, 0.77	-24.43	-21.52	-21.33	-23.59	-21±6
		Empe.1	-21.44				
		Empe.2	-12.06				
25, 47	$5/2^-$	1.15, 0.75	29.75	26.36	26.04	28.80	30.2±10
		Empe.1	26.36				
		Empe.2	14.39				
26, 48	2^+	B-M 1.14, 0.73	-60.23	-17.33	-49.15	-18.87	-17.7±8
		Empe.1	-51.72				
		Empe.2	-23.70				
27, 49	$7/2^-$	B-M 1.13, 0.71	25.39	23.10	22.72	25.13	24.7 ±11
		Empe.1	23.17				
		Empe.2	12.26				
28, 50	2^+	B-M 1.12, 0.69	4.14	3.46	3.28	3.64	8±16
		Empe.1	3.58				
		Empe.2	1.37				
30, 52	2^+	B-M 1.10, 0.65	-7.19	-7.13	-7.08	-7.84	
		Empe.1	-7.09				
		Empe.2	-4.05				

3.2. Electric quadrupole moments

Theoretical electric quadrupole moments ' $Q.M_{th}$ ' were calculated for the $^{43,44,45,46,47,48,49,50,52}\text{Ti}$ isotopes using different effective charges. Various different effective charges are adopted in the present work, the first being the Bohr-Mottelson effective charges (B-M) [8, 14] which is calculated according to equation (13) for each isotope, and as reported in table 2. Figure 2 shows the theoretical quadrupole moments calculated for all the selected Ti isotopes in comparison with

the available experimental data. Inspection of these curves reveals that calculated values for the ^{43}Ti ($N = 21, 19/2^-$) isotope were underestimated compared to the experimental data. These values indicated in the ^{43}Ti nucleus was predicted to be oblate with a neutron number of $N = 21$. The theoretical values for the quadrupole moments ' $Q.M_{th}$ ' for ^{44}Ti ($N = 22, 2^+$) were calculated using different effective charges. These values indicate the oblate deformation in the ^{44}Ti nucleus; unfortunately, the experimental data for this nucleus is unavailable, and needs further investigation. The $Q.M_{th}$ for ^{45}Ti

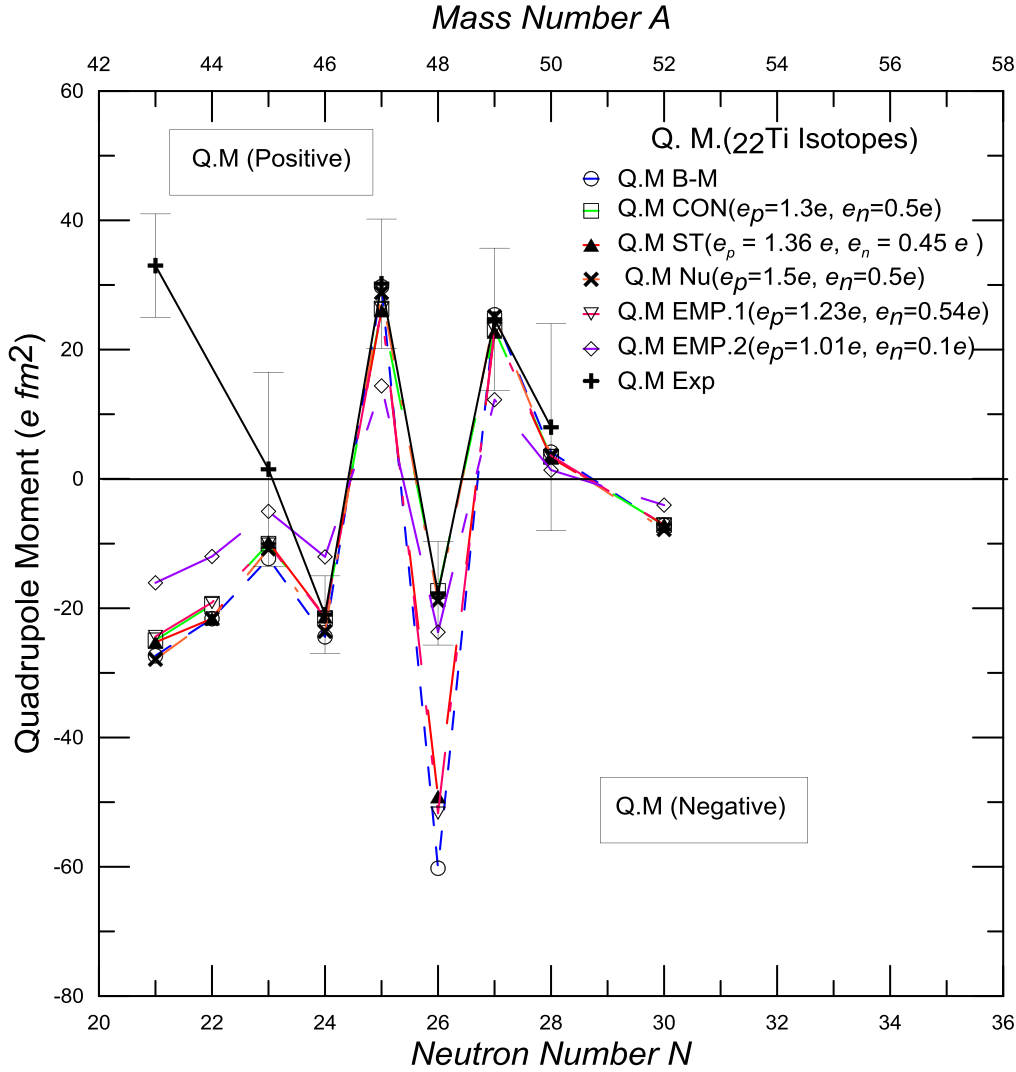


Figure 2. The theoretical calculated values for the quadrupole moments $Q.M_{th}$ (units of $e \text{ fm}^2$) for the $^{43,44,45,46,47,48,49,50,52}\text{Ti}$ ($Z = 22$) isotopes and the experimental electric quadrupole moments (measured) $Q.M_{exp}$ are taken from [13]. The B-M effective charges [14], CON (Con ($e_p = 1.3 e$, $e_n = 0.5 e$) [15], the ST ($e_p = 1.36 e$, $e_n = 0.45 e$) [16], are from the NushellX program ($e_p = 1.5 e$, $e_n = 0.5 e$) [17], the Emp.1 ($e_p = 1.23 e$, $e_n = 0.54 e$), and the Emp.2 effective charges ($e_p = 1.01 e$, $e_n = 0.1 e$).

($N = 23$, $7/2^-$) were calculated, and were found to be in agreement with $Q.M_{exp}$ [13] within the bounds of the associated errors. These values indicate the ^{45}Ti nucleus has an oblate shape. The $Q.M_{th}$ calculated for ^{46}Ti ($N = 24$, 2^+) were close to the associated $Q.M_{exp}$, again within experimental error bounds, except for the $Q.M_{th}$ determined using the Emp.2 effective charges, which overestimated the $Q.M_{exp}$. The results further indicate that the ^{46}Ti nucleus is oblate, where the four neutrons are distributed in $1f_{7/2}$ orbit. The $Q.M_{th}$ calculated for the ^{47}Ti ($N = 25$, $5/2^-$, stable) isotope were in agreement with $Q.M_{exp}$ [13] within the bounds of experimental error, again with the exception of that determined using Emp.2 effective charges, which underestimates the experimental $Q.M_{exp}$. The nucleus in this case shows a prolate deformation, and with five neutrons distributed in the $1f_{7/2}$ orbit. The $Q.M_{th}$ calculated for the ^{48}Ti ($N = 26$, 2^+) isotope using, CON, NS, and Emp.2 effective charges were all close to the experimentally determined values; of $Q.M_{exp}$. However, the results using, B-M, ST, and Emp.1 effective

charges overestimated the experimental data. These results indicated a large oblate deformation for this particular nucleus. The $Q.M_{th}$ for the ^{49}Ti ($N = 27$, $7/2^-$, stable) isotope was in line with $Q.M_{exp}$ [13] within the bounds of experimental error, where nine neutrons are distributed in $1f_{7/2}$ and $2p_{3/2}$ orbits. However, the $Q.M_{th}$ determined using Emp.2 effective charges is close to the experimental data. The $Q.M_{th}$ values calculated for the ^{50}Ti ($N = 28$, 2^+) isotope, were close to the associated experimental data of $Q.M_{exp}$ [13] within the bound of experimental error. The above indicates a prolate deformation although the number of neutrons ($N = 28$) is a magic number. Here, the shell closure collapses magicity and the disappearance of magicity for $N = 28$ (magic number) progressively with spherical shell closures. Calculations using the shell model indicate that ^{50}Ti is best described as having a small deformed prolate shape. The $Q.M_{th}$ values calculated for the ^{52}Ti ($N = 30$, 2^+) isotope, (using all effective charges) cannot be compared experimental data. This isotope shows an oblate deformation in the nucleus

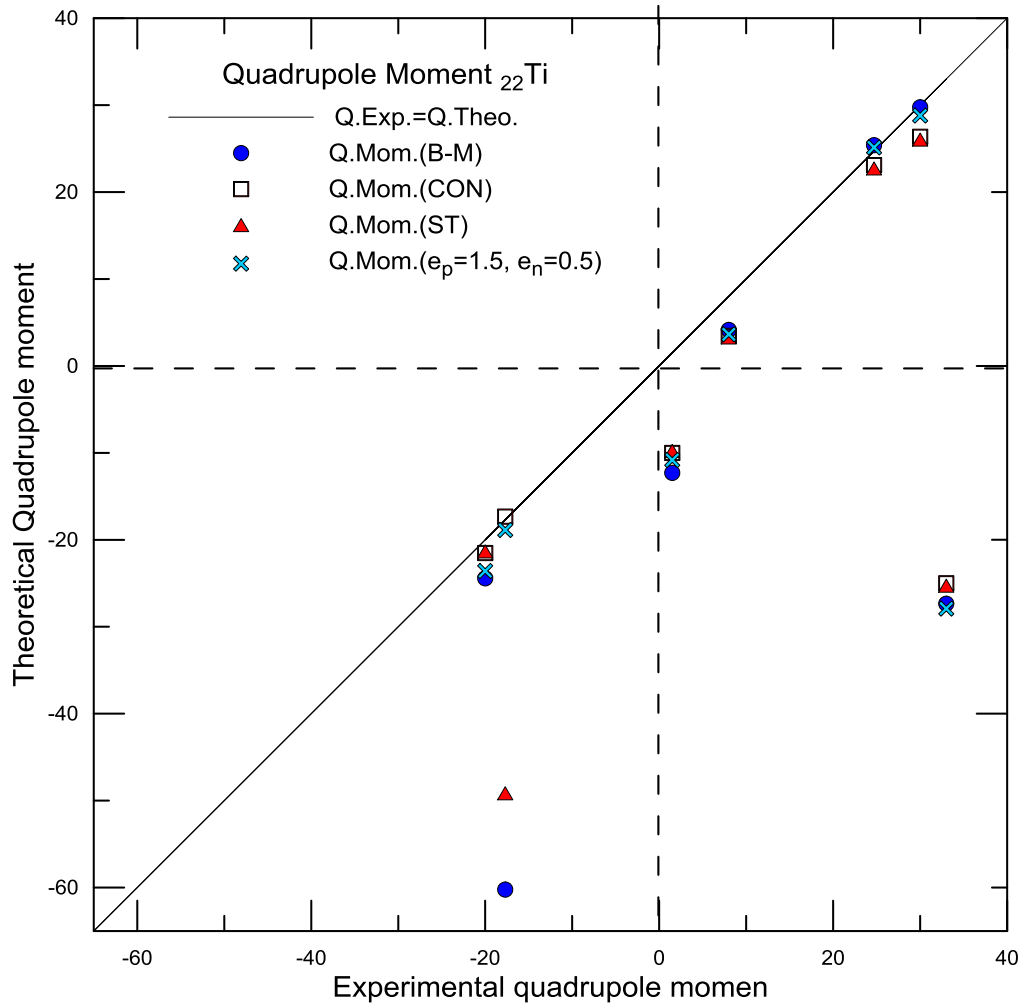


Figure 3. Comparison between the calculated (theoretical) and experimental (taken from [13]) quadrupole moments for isotopes Ti ($Z = 22$, $A = 43, 44, 45, 46, 47, 48, 49, 50, 52$) with several effective charges, such as B-M, CON, ST and with the effective charges from the NushellX program (Nu) $e_p = 1.5e$ and $e_n = 0.5e$ [17]. The straight line represents the line $Q_{\text{exp}} = Q_{\text{theo}}$.

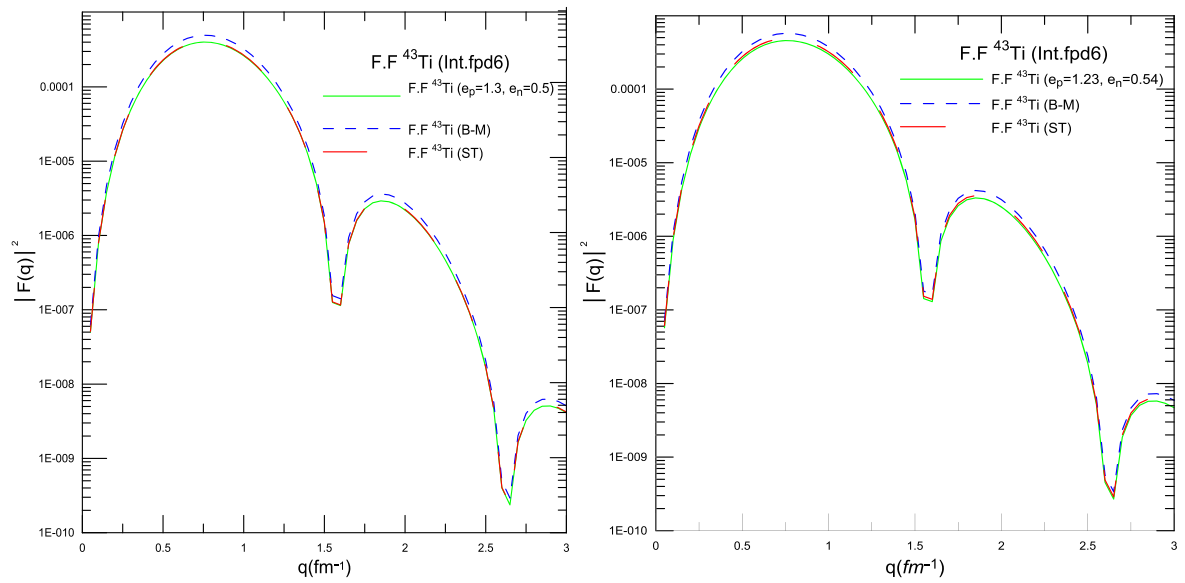


Figure 4. The form factors for ^{43}Ti using different effective charges, Experimental data are not available.

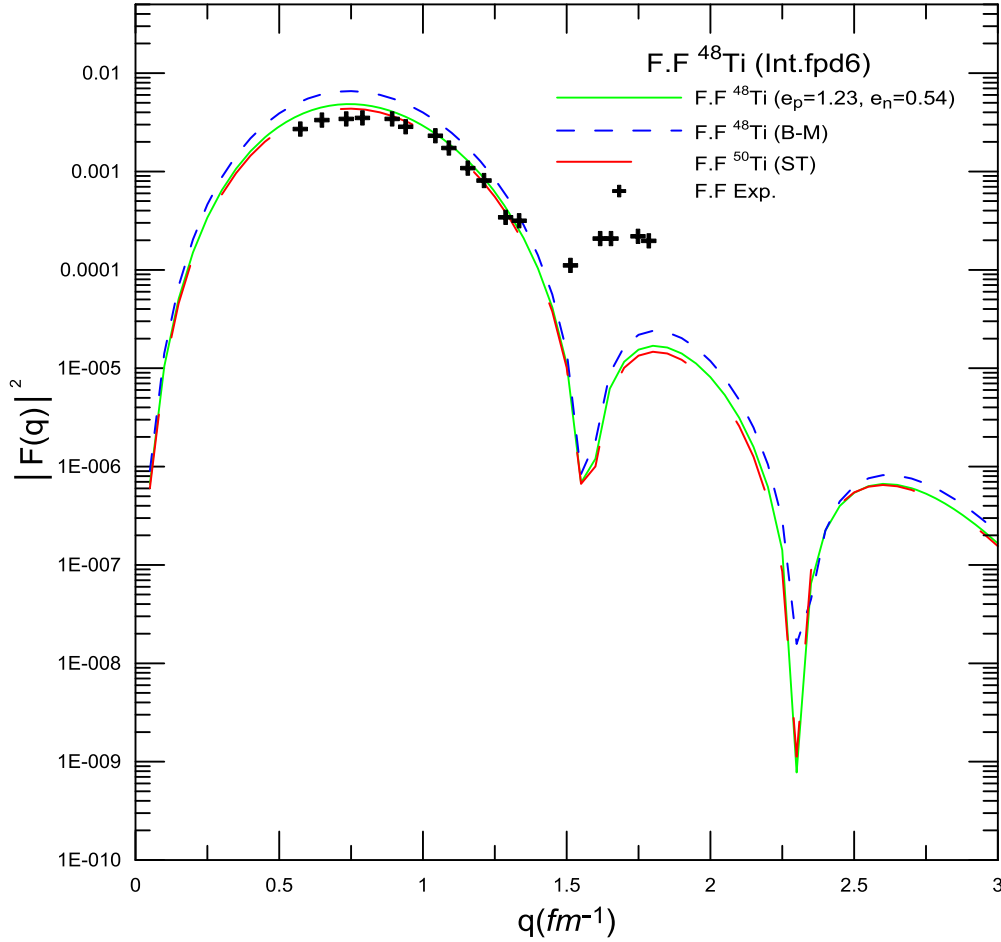


Figure 5. Comparison between the theoretical calculated and experimental of form factors for ^{48}Ti . Experimental values are taken [19].

which has the neutrons ($N \geq 20$) distributed in $1f_{7/2}$ and $2p_{3/2}$ orbits, as shown in table 2 and figure 2.

Figure 3 shows a comparison between the calculated (theoretical) and experimental data of the quadrupole moments using several different effective charges. The straight line represents the experimental data of Q_{exp} being equal to the calculated values (theoretical) of Q_{theo} , where the better theoretical values, that is, the closest to the straight line ($Q_{\text{exp}} = Q_{\text{theo}}$), were determined using the Nu and CON effective charges.

3.3. Elastic longitudinal electron scattering form factors

Elastic longitudinal electron scattering form factors for the $^{43,48,50}\text{Ti}$ isotopes have been calculated using different nuclear effective charges, the result of which are presented in figures 4–6, respectively. These calculations are performed using the *fpd6* effective interaction for the *fp*-shell model space to generate the OBDM elements. As mentioned previously, the wave functions for single-particle matrix elements were calculated using an HO potential [18]. Figure 4 shows the behaviour of the form factor for the ^{43}Ti ($J^\pi = 19/2^-$) isotope using different effective charges. Unfortunately, there is no available experimental data for this

isotope. For the $^{48,50}\text{Ti}$ isotopes, the elastic longitudinal electron scattering form factors are depicted in figures 5 and 6. For the $^{48,50}\text{Ti}$ ($J^\pi = 2^+$) isotopes, it is clear that the calculated form factors are in a good agreement with experimental data [19] using the ST effective charge in the low momentum transfer region, but with the deviation progressively increasing and ultimately overestimating the experimental values. The form factor for ^{50}Ti isotope is shown in figure 6 in comparison with the experimental data taken from [20]. It is obvious that the calculated form factors are in reasonable agreement with the general trend of the experimental data although the calculated form factors underestimate the experimental values for the momentum transfer region up to $q < 1 \text{ fm}^{-1}$ and overestimate the experimental values for the region up to $q > 2.5 \text{ fm}^{-1}$. However, they were close to the experimental values for $q < 2.5 \text{ fm}^{-1}$.

4. Conclusions

Magnetic dipole moments, quadrupole moments, and form factors for various isotopes of Ti were calculated using the *fpd6* interaction, as were magnetic dipole moments by the inclusion of the core polarization with effective free nucleon g

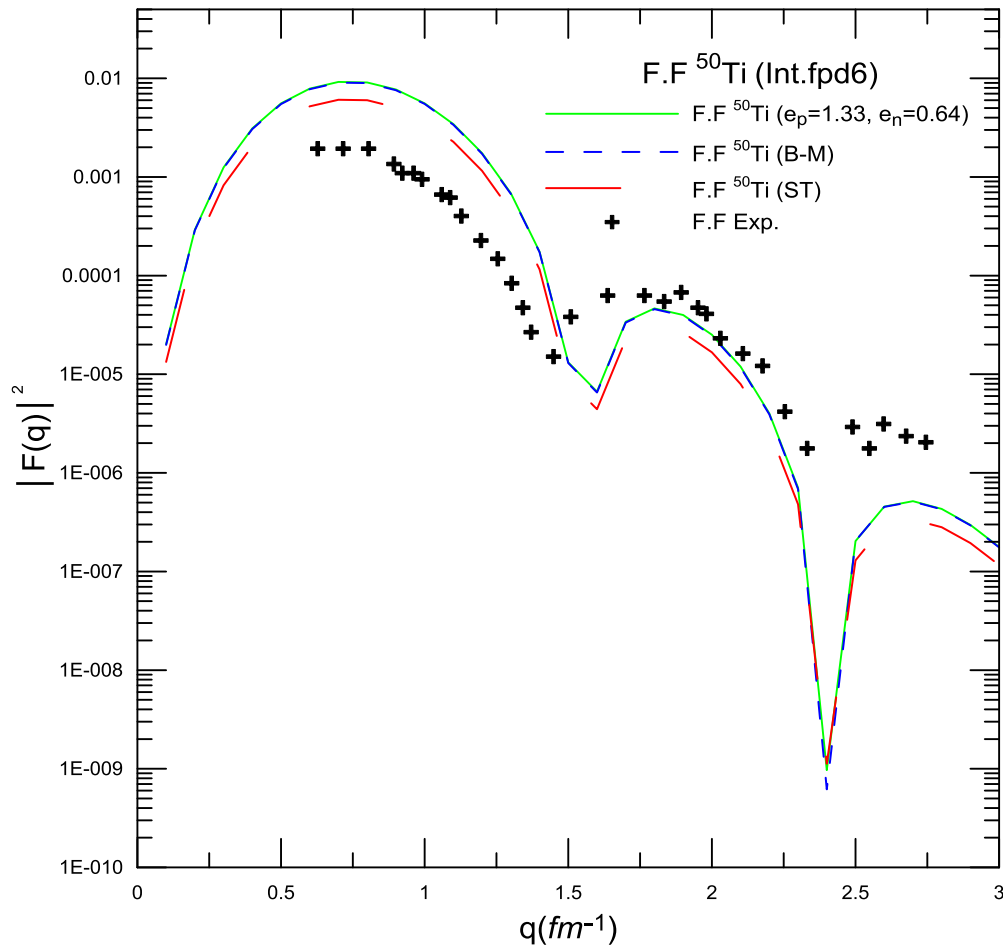


Figure 6. Comparison between the theoretical calculated and experimental of form factors for ^{50}Ti . Experimental values are taken [20].

factors and effective nucleon g factors. The magnetic dipole moments calculations using the free nucleon g factors and the effective nucleon g factors were in good agreement within the bounds of error, with the experimental data for $^{43,44,46,47,48,49,50}\text{Ti}$ isotopes, while the magnetic dipole moments calculated underestimated the experimental data for $^{45,52}\text{Ti}$ isotopes. The calculations of quadrupole moments were performed by using the inclusion of the core polarization with effective charges. The quadrupole moment calculations were performed using the B-M, Con ($e_p = 1.3e$, $e_n = 0.5e$), ST ($e_p = 1.36e$, $e_n = 0.45e$), Nu ($e_p = 1.5e$, $e_n = 0.5e$), Emp1 ($e_p = 1.23e$, $e_n = 0.1e$), Emp2 ($e_p = 1.01e$, $e_n = 0.1e$) and the *fpd6* interactions. The theoretical quadrupole moments for the $^{45,46,47,49,50}\text{Ti}$ isotopes, as found using various effective charges, were in excellent agreement with experiment, with the exception of $^{46,47}\text{Ti}$ using Emp2. The theoretical quadrupole moments for ^{48}Ti are in agreement with the experimental data when using the CON and NU effective charges. We can deduce that the magicity of ^{50}Ti ($N = 28$) shell closure is progressively vanishing, with the nucleus appearing as a small deformed a prolate shape. The best results for the theoretical quadrupole moments were obtained from Con and Nu effective charges using the *fpd6* interaction. The behaviour of the form factors has been studied for various isotopes Ti using different effective charges

and the *fpd6* interaction. The form factors for $^{48,50}\text{Ti}$, when using the core polarization, have constructive and enhancement properties, with the results so obtained being in close agreement with the experimental values for ^{48}Ti . However, the results were not in such good agreement in the low momentum transfer q region for ^{50}Ti , and more in the region of high momentum transfer q . This implies that further theoretical efforts are needed to examine this state.

ORCID iDs

Ahmed H Ali  <https://orcid.org/0000-0002-1525-1406>

References

- [1] Neyens G 2003 Nuclear magnetic and quadrupole moments for nuclear structure research on exotic nuclei *Rep. Prog. Phys.* **66** 633–89
- [2] Carchidi M, Wildenthal B H and Brown B A 1986 Quadrupole moments of sd-shell nuclei *Phys. Rev. C* **34** 2280
- [3] Soloviev V G 1976 *Theory of Complex Nuclei* (Oxford: Pergamon)

- [4] Richter W A, Merwe M G, Julies R E and Brown B A 1991 New effective interactions for the $0f_{7/2}$ shell *Nucl. Phys. A* **523** 325
- [5] Sick I 2001 Elastic electron scattering from light nuclei *Prog. Part. Nucl. Phys.* **47** 245
- [6] Yennie D R, Ravenhall D G and Wilson R N 1954 Phase-shift calculation of high-energy electron scattering *Phys. Rev.* **95** 500
- [7] Brussaard P and Glaudemans P 1977 *Shell-Model Applications in Nuclear Spectroscopy* (Amsterdam: North Holland Publishing Comp) p 452
- [8] Radhi R A, Alzubadi A A and Ali A H 2018 Magnetic dipole moments, electric quadrupole moments, and electron scattering form factors of neutron-rich sd - pf cross-shell nuclei *Phys. Rev. C* **97** 1–13
- [9] Radhi R A, Alzubadi A A and Ali A H 2017 Calculations of the quadrupole moments for some nitrogen isotopes in p and psd shell model spaces using different effective charges *Iraqi J. Sci.* **58** 878–83
- [10] de Forest T Jr and Walecka J D 1966 Electron scattering and nuclear structure *Adv. Phys.* **15** 1
- [11] Brown B A and Rae W D M 2014 The shell-model code NuShellX@MSU *Nucl. Data Sheets* **120** 115–8
- [12] Brown B A, Radhi R and Wildenthal B H 1983 Electric quadrupole and hexadecapole nuclear excitations from the perspectives of electron scattering and modern shell-model theory *Phys. Rep.* **101** 313
- [13] Stone N J 2014 Table of nuclear magnetic dipole and electric quadrupole moments *International Data Committee*. (International Atomic Energy Agency (IAEA), INDC (NDS)) 171 (<https://www-nds.iaea.org/publications/indc/indc-nds-0658.pdf>) (https://inis.iaea.org/search/search.aspx?orig_q=RN:45029196)
- [14] Bohr A and Mottelson B R 1975 *Nuclear Structure* (New York: Benjamin) vol 2, p 515
- [15] Brown B A and Wildenthal B H 1988 Status of the nuclear shell model *Ann. Rev. Nucl. Part. Sci.* **38** 29
- [16] Richter W A, Mkhize S and Brown B A 2008 Sd -shell observables for the USDA and USDB hamiltonians *Phys. Rev. C* **78** 064302
- [17] Klose A *et al* 2019 Ground-state electromagnetic moments of ^{37}Ca *Phys. Rev. C* **99** 06130
- [18] Ali A H 2020 Investigation of the quadrupole moment and form factors of some Ca isotopes *BS J.* **17** 508
- [19] Sahu R, Ahalpara D P and Bhatt K H 1990 Inelastic electron scattering from fp -shell nuclei *J. Phys. (London)* **G16** 733
- [20] Salman A D, Adeeb N M and Oleiwi M H 2013 Core polarization effects on the inelastic longitudinal C_2 and C_4 form factors of $^{46,48,50}\text{Ti}$ nuclei *Journal of Nuclear and Particle Physics* **3** 20–4